Demonstration of Secondary Currents in the Pressure-Driven Flow of a Concentrated Suspension Through a Square Conduit

Adam Zrehen and Arun Ramachandran

Department of Chemical Engineering and Applied Chemistry, University of Toronto, Toronto, Ontario, Canada M5S3E5

(Received 7 May 2012; revised manuscript received 9 November 2012; published 3 January 2013)

The existence of secondary flows in the pressure-driven flow of a concentrated suspension of noncolloidal particles through a conduit of square cross section under creeping flow conditions is confirmed experimentally. This Letter lends support to the idea that secondary currents, rather than shear-induced migration, may actually be the dominant mechanism that determines particle distribution in noncolloidal suspension flows through nonaxisymmetric geometries. This work also establishes that coextrusion of two concentrated suspensions through nonaxisymmetric geometries with a stable suspension-suspension interface is not possible, except in special situations.

DOI: 10.1103/PhysRevLett.110.018306 PACS numbers: 83.80.Hj

When a viscoelastic polymer is subjected to a simple shear flow, normal stresses are developed in each of the principal directions [flow (1), gradient (2), and vorticity (3)] due to the stretching of the polymer by the flow [1]. These stresses are characterized by the first normal stress difference, $N_1 = \Sigma_{11} - \Sigma_{22}$, and the second normal stress difference, $N_2 = \Sigma_{22} - \Sigma_{33}$. For polymers, N_1 is positive, and manifests itself in well-documented and recognized ways, such as rod climbing, die swell, etc., [1]. On the other hand, N_2 in polymers is negative, and weak in magnitude relative to N_1; nevertheless, it is known to produce some subtle effects. For example, it has been known since the 1950s that pressure-driven flow of polymer melts and solutions in nonaxisymmetric conduits cannot be unidirectional [2–4]; the main flow through the channel is accompanied by secondary currents, whose origin can be attributed to N_2. Thus, the flow of a viscoelastic polymer through the channel is effectively a helicoidal flow.

Only recently [5] was it realized that secondary currents may also exist in pressure-driven flows of concentrated suspensions of rigid particles in Newtonian fluids, because, akin to polymeric fluids, suspensions also exhibit N_2 in simple shear flows [6–8]. The origin of N_2 in suspensions is not elasticity, but rather the anisotropic particle microstructure [9–13]. In suspensions, N_2 has been experimentally determined to be negative, directly proportional to the magnitude of the shear stress, monotonically increasing with the volume fraction of the particles, and independent of the particle size in the noncolloidal limit [6–8].

Secondary currents in suspension flows have a special implication as compared to polymer flows, in that they are capable of influencing the spatial particle distribution in the flow. Traditionally, the mechanism considered in describing particle distributions in flowing suspensions is shear-induced migration [14–16], which causes particles to migrate from regions of high shear stresses to low, high concentrations to low and high streamline curvatures to low, and high streamline curvatures to low. Secondary currents are weak relative to the average velocity of the suspension in the channel; however, the magnitude of secondary currents relative to the characteristic velocities associated with shear-induced migration scales as B^2/a^2, where B is the characteristic dimension of the channel and a is the particle radius. Since the value of B^2/a^2 in most suspension flows is large (100 or more), secondary currents may be the dominant mechanism determining the particle distribution in flowing suspensions.

Inclusion of secondary currents in suspension flow calculations produces some interesting and counterintuitive predictions: dependence of fully developed concentration distributions in neutrally buoyant suspension flows on particle size, quantitative description of resuspension of non-neutrally-buoyant particles in tube flow [17–19] (previously impossible to explain with isotropic models), depletion of particles from corners and notches of geometries in pressure-driven suspension flow (which is consistent with recent confocal microscopy measurements [20]), and instabilities even in such simple geometries as plane Poiseuille flow [5,21]. But in spite of all these potentially interesting and counterintuitive effects, there is no direct experimental evidence of secondary currents for suspension flow in nonaxisymmetric conduits. The objective of this work is to remedy that deficiency. We perform pressure-driven flow of concentrated suspensions through a conduit of square cross section to demonstrate the existence of secondary currents, and interrogate the dependence of these currents on particle size, flow rate, and particle volume fraction.

The experimental setup is shown in Fig. 1. A square tube of internal side length 1 cm is oriented vertically, i.e., with its axis parallel to gravity (z direction). The flow or the (1) direction in this geometry is along the z axis, while the (2) and (3) directions are in the cross-sectional (x-y) plane. The tube has two ports for supplying suspension: a bottom port that receives suspension at a flow rate Q_m, and a smaller front port [see Fig. 1(a)] on the front x-z plane that receives suspension at a much lower flow rate Q_s.

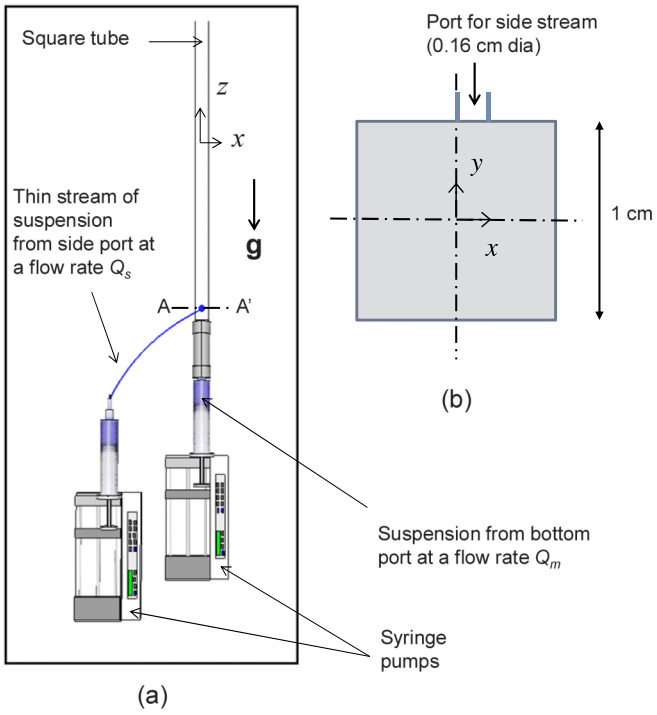

FIG. 1 (color online). Experimental setup. (a) Front view (x-z plane). (b) Cross-sectional view (x-y plane) across segment $A - A'$ in (a).

The front port is placed asymmetrically on the right half of the cross section [see Fig. 1(b)]. The two suspensions are identical in all respects except for the color of the dye in the suspending fluid; the suspension from the bottom is dyed yellow, while the one from the front port is dyed blue. The base suspending fluid, a mixture of 81 wt% Karo syrup, 18 wt% glycerin, and 1 wt% water, is Newtonian with a viscosity of 22.5 poise at 23 °C, and has a density of 1.35 gm/cm^3. Blue or yellow food coloring (Durkee) is added at a volume ratio of 1 part dye to 40 parts fluid. The particles in the suspension are glass spheres (Mo-Sci Corp., class V, density = 2.5 gm/cm^3). Most of our experiments have been performed using 46 ± 3 μm glass spheres, but we have used 94(±5) μm particles in some experiments to examine the effect of particle size. Similarly, the particle volume fraction ϕ in almost all experiments was 40%; the experiments at 30% were performed to understand the effect of volume fraction. The experimental parameters have been carefully selected to suppress shear-induced migration [22] and buoyancy effects [23]. The interface between the two contrastingly dyed suspensions in the x-z plane under fully developed flow conditions was photographed at regular intervals in height using a camera mounted on a vertical linear stage. These images were stitched together to reveal the progression of the blue suspension in the bulk flow of the yellow suspension.

The results from these experiments are shown in Fig. 2. In Fig. 2(a), we present the result from a control experiment where only pure fluids (no particles) were used. It can

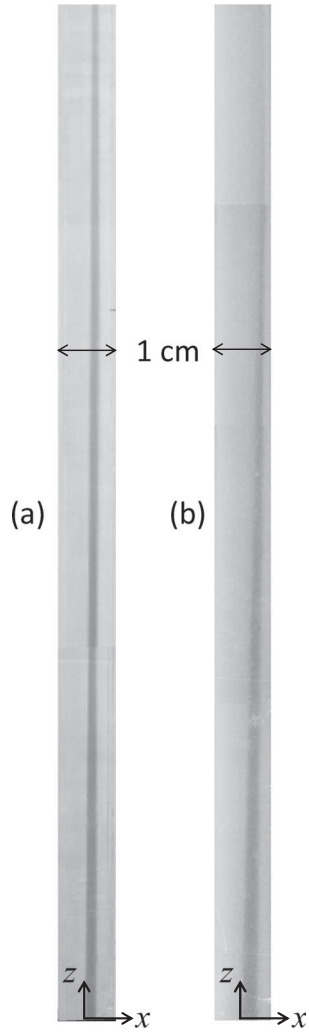

FIG. 2. Photographs of the front (x-z) view of the experiment with coflowing (a) pure fluids ($Q_m/Q_s = 32$ with Q_m = 8 ml/min) and (b) suspensions ($\phi = 0.4$, $2a = 46$ μm, and $Q_m/Q_s = 30$ with $Q_m = 6$ ml/min). Both photographs preserve the true aspect ratio, with the channel width being 1 cm.

be seen that the interface between the blue (dark) and yellow (light) suspension streams is straight; there is no deviation from rectilinearity. This is consistent with our expectations, since no secondary currents are predicted for particle-free, coflowing streams at low Reynolds numbers. Figure 2(b) shows the result for a 40%, 46 μm particle diameter suspension at a flow rate ratio Q_m/Q_s of 30 with $Q_m = 6$ ml/min. The stripe of blue suspension deviates to the right, becomes thinner and eventually vanishes. These pictures clearly indicate that the motion of the suspension through a square conduit is not unidirectional; the main flow along the axis of the conduit is accompanied by secondary currents.

Let us now determine if this pattern can be explained by the non-Newtonian rheology of suspensions. Since shear-induced migration effects are negligible in our geometry [22] and the suspension is homogeneous at the inlet, we

can assume that the concentration distribution within the channel is uniform. Using the theoretical development by Ramachandran and Leighton [5], the equations governing the velocity field $[u, v, w]$ in the $[x, y, z]$ directions can be written as

$$u_x + v_y = 0, \qquad \nabla^2 w = -\frac{1}{\mu_r}, \tag{1a}$$

$$\nabla^2 u - \frac{\tilde{P}_x}{\mu_r} = \alpha d\left[\frac{\partial}{\partial x}\left(\frac{w_y^2}{\dot{\gamma}}\right) - \frac{\partial}{\partial y}\left(\frac{w_x w_y}{\dot{\gamma}}\right)\right], \tag{1b}$$

$$\nabla^2 v - \frac{\tilde{P}_y}{\mu_r} = \alpha d\left[-\frac{\partial}{\partial x}\left(\frac{w_x w_y}{\dot{\gamma}}\right) + \frac{\partial}{\partial y}\left(\frac{w_x^2}{\dot{\gamma}}\right)\right]. \tag{1c}$$

Here, P is a pressure that has been adjusted for the constant pressure gradient driving the flow, $\alpha = 2.17\phi^3 \exp(2.34\phi)$ is a reduced normal stress, $d = -0.54$ is the coefficient of the reduced second normal stress difference, $\mu_r = \exp(-2.34\phi)/(1 - \phi/0.62)^3$ is the suspension relative viscosity, and $\dot{\gamma} = \sqrt{w_x^2 + w_y^2}$ is the local shear rate. The lengths have been rendered dimensionless with respect to the half-width of the cross section, while velocities have been rendered dimensionless with respect to the viscous scaling based on the constant pressure gradient in the fully developed flow. The no-slip boundary condition is imposed on the walls of the cross section due to the large aspect ratios ($B/a > 100$) and the moderate volume fractions in our experiments [24].

The velocity field calculated using the above equations is shown in Fig. 3 in the first quadrant of the cross section. One can see that secondary currents flow out of the corners along the diagonal, then along the symmetry axis to the edge of the cross section, and then back along the edge to the corner. There are eight such circulation cells in the entire cross section. In the experiments, we introduce a thin stream of the second suspension just below the edge of the square cross section. If we assume that the suspension introduced in this way is in the form of a rectangular patch,

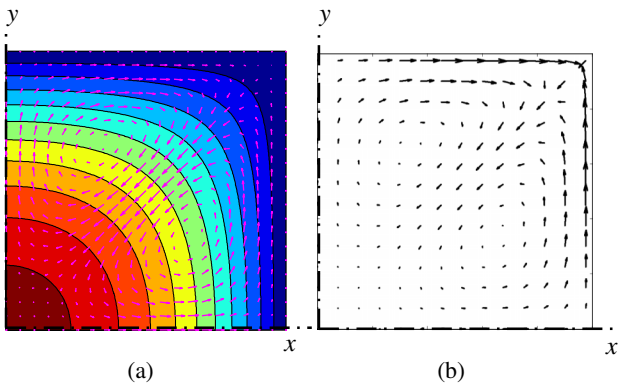

FIG. 3 (color online). Velocity profile for suspension flow at uniform concentration. (a) Contours—axial flow $w/\langle w\rangle$ [red, maximum velocity; blue, $w = 0$], Arrows—secondary currents $[u/\langle w\rangle, v/\langle w\rangle]$. (b) Arrows—secondary currents $[u/w, v/w]$. Only the first quadrant of the cross section is shown.

every material point (x_g, y_g) in the patch evolves in the axial direction according to the equation

$$\frac{dx_g}{dz} = \frac{u(x_g, y_g)}{w(x_g, y_g)}, \qquad \frac{dy_g}{dz} = \frac{v(x_g, y_g)}{w(x_g, y_g)}. \tag{2}$$

The equations are solved in MATLAB using the Euler explicit scheme and an adaptive mesh, and the results are shown in Fig. 4. It may be seen that the patch stretches and distorts as it moves towards the corner of the square cross section, and is ultimately swept into the interior of the cross section. In the experiment, the images can only reveal information over a limited depth below the top edge of the square cross section due to the opacity of the suspension. Therefore, the stripe appears to have disappeared from the field of view after propagating in the axial direction for a certain distance. The pattern of motion of the blue suspension stripe observed in the experiment is thus qualitatively consistent with theory.

We now ascertain whether the variations in the experiment results with the particle size, the total flow rate, and the particle volume fraction are consistent with expectations from scaling arguments. From the governing equations (1), we can deduce the velocity scale, U_s of the secondary currents as $U(-d)\alpha$, where U is the average velocity of the

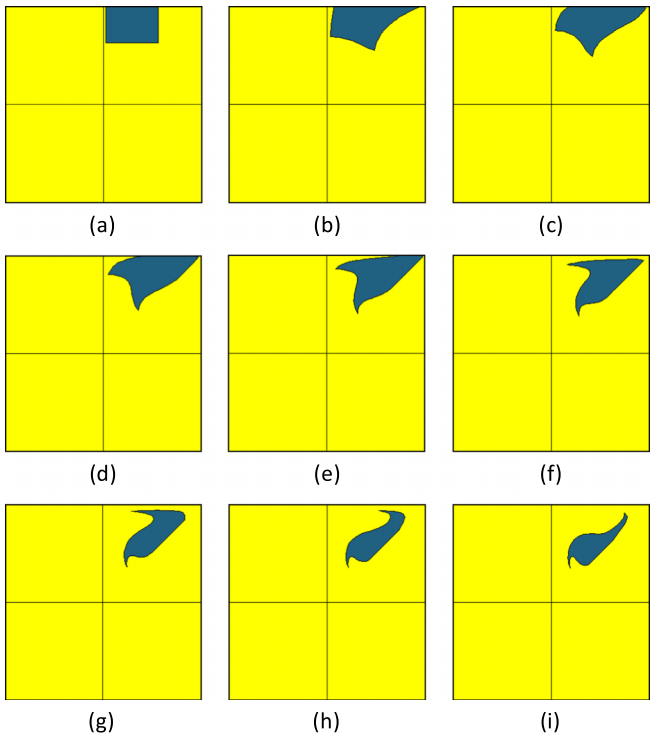

FIG. 4 (color online). Prediction of the cross-sectional evolution of a patch of blue (dark) suspension in a stream of yellow suspension in a square tube of side 1 cm for $\phi = 0.4$. The area and position of the blue patch are chosen so that its flow rate is a factor of 1/32 relative to the flow rate of the yellow fluid. Panels (a)–(i) show the shapes of the patch within the cross section from 0 to 80 cm in steps of 10 cm.

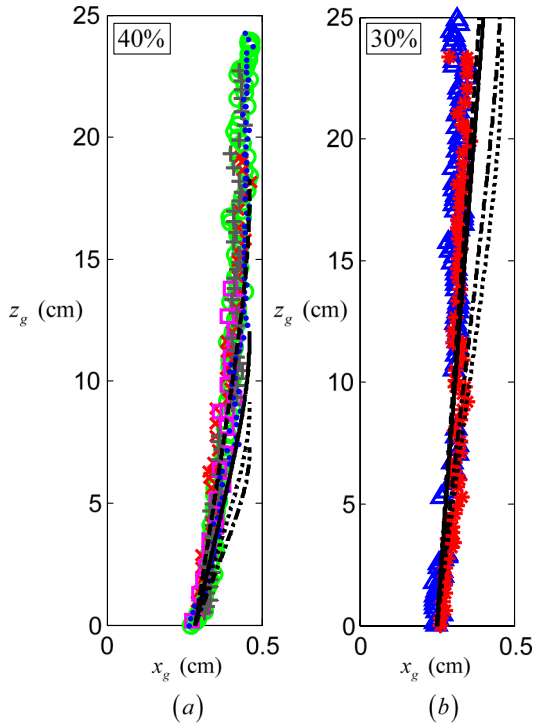

FIG. 5 (color online). The x_g-z_g trajectory of the right edge of the stripe of blue fluid observed in the front view [see Fig. 1(a)] starting at $x_g \approx 0.26$. (a) 40% data. (Open circle) $2a = 94$ μm, $Q_m = 8$ ml/ min, $Q_m/Q_s = 32$; (crosses) $2a = 46$ μm, $Q_m = 6$ ml/ min, $Q_m/Q_s = 30$; (open square, plus symbol) $2a = 46$ μm, $Q_m = 8$ ml/ min, $Q_m/Q_s = 64$. (b) 30% data. (Asterisk) $2a = 94$ μm, $Q_m = 8$ ml/ min, $Q_m/Q_s = 16$, (open upward triangle) $2a = 46$ μm, $Q_m = 8$ ml/ min, $Q_m/Q_s = 64$. The solid, dash-dotted, dashed and dotted lines are the theoretical predictions using the models of Refs. [6–8,25], respectively.

flow through the cross section. Since $U_s \propto U$, the path traced by a material point in the flow through the channel is expected to be independent of the flow rate through the channel. The scaling also indicates that this trajectory should be unaltered by the particle radius a. The only experimental parameter that should affect the path of a material point is the volume fraction of the suspension, through the reduced normal stress α.

The material point that we have chosen to track is the right edge of the blue (dark) suspension stripe in the images. We choose not to track the left edge, because, as may be seen in Fig. 3, the left edge as viewed from the top of the channel may not always correspond to the same material point. In Fig. 5, we have shown a plot of x_g, the x position of the right edge against the variable z_g, where z_g is the vertical position of the right edge, for different particle sizes, flow rates, and flow rate ratios (Q_m/Q_s) for 30% and 40% suspensions. The trajectories for all experimental data sets have been corrected in the z direction by a constant, so that every data set begins at $x_g = 0.26$ at $z_g = 0$. We see that all data at 40% fall on a single master curve, independent of a, Q_m, ϕ, and Q_m/Q_s. The data at 30% evolve much more slowly in the z direction than that at 40%. This is expected, because the secondary currents become weaker as the volume fraction is decreased. Also shown is the x-z evolution of the material point expected from the solution of the equations in Eq. (2) (solid curves), which employ the constitutive equations of Zarraga *et al.* [6]. In addition, we have compared the results with the same momentum equations, but with the constitutive models of Couturier *et al.* [8] (dotted line), Singh and Nott [7] (dash-dotted line), and Morris and Boulay [25] (dashed line). We see that agreement is good with all the constitutive models for short distances [26]. But, eventually the magnitude of the secondary currents is overpredicted, and the material point appears to reach the corner over much shorter distances as compared to experiments. A factor we think leads to this discrepancy is that, near the walls and the corner, the flow is more complicated than a perturbation of a simple shear flow, an assumption built into the development of Eq. (1) [5]. A comprehensive framework for modeling suspension motion in arbitrary flow geometries is, however, yet to be developed and verified by experiment.

The consistency of the observed secondary currents with the expected pattern and scaling arguments lends support to the predictions of secondary-current-influenced particle distributions in the work of Ramachandran and Leighton [5]. This work should motivate experimental measurements of concentration distributions in nonaxisymmetric geometries in which fluxes due to shear-induced migration and secondary currents are both important. Additionally, our work suggests a revisit of past experimental studies in nonaxisymmetrc geometries to examine if secondary currents [20,27,28] could have influenced the results in those investigations. We are currently also investigating the potential augmentation of the mass transfer rate of solutes in flowing, concentrated suspensions arising due to secondary currents; this has strong implications for the mass transfer of macromolecules in blood flow. Finally, a direct conclusion from this work is that the production of a stable coextrudate by combining two concentrated, particulate suspensions is, in general, not possible, and this is explained in the Supplemental Material [29] via an experimental demonstration in a rectangular conduit. Coextrusion of neutrally-buoyant suspensions can be implemented only under special circumstances, e.g., (a) for axisymmetric geometries, where secondary currents are absent, (b) for nonaxisymmetric geometries, when the flow rates and the locations of introduction of the two suspension streams preserve the symmetry of the secondary current cells.

[1] R. B. Bird, R. C. Armstrong, and O. Hassager, *Dynamics of Polymeric Liquids* (Wiley-Interscience, New York, 1987).
[2] J. L. Ericksen, Q. Appl. Math. **14**, 318 (1956).

[3] A. E. Green and R. S. Rivlin, Q. Appl. Math. **14**, 229 (1956).
[4] H. Giesekus, Rheol. Acta **4**, 85 (1965).
[5] A. Ramachandran and D. T. Leighton, J. Fluid Mech. **603**, 207 (2008).
[6] I. E. Zarraga, D. A. Hill, and D. T. Leighton, J. Rheol. **44**, 185 (2000).
[7] A. Singh and P. R. Nott, J. Fluid Mech. **490**, 293 (2003).
[8] E. Couturier, F. Boyer, O. Pouliquen, and E. Guazzelli, J. Fluid Mech. **686**, 26 (2011).
[9] F. Parsi and F. Gadala-Maria, J. Rheol. **31**, 725 (1987).
[10] I. Rampall and D. T. Leighton, *Particulate and Multiphase Flow* (Butterworth-Heinemann, Boston, 1993), pp. 190–208.
[11] J. F. Brady and J. F. Morris, J. Fluid Mech. **348**, 103 (1997).
[12] D. R. Foss and J. F. Brady, J. Fluid Mech. **407**, 167 (2000).
[13] C. Gao, S. D. Kulkarni, J. F. Morris, and J. F. Gilchrist, Phys. Rev. E **81**, 041403 (2010).
[14] D. Leighton and A. Acrivos, J. Fluid Mech. **181**, 415 (1987).
[15] A. Acrivos, J. Rheol. **39**, 813 (1994).
[16] J. F. Morris, Rheol. Acta **48**, 909 (2009).
[17] S. A. Altobelli, R. C. Givler, and E. Fukushima, J. Rheol. **35**, 721 (1991).
[18] A. Ramachandran and D. T. Leighton, Phys. Fluids **19**, 053301 (2007).
[19] A. Ramachandran and D. T. Leighton, J. Rheol. **51**, 1073 (2007).
[20] C. Gao and J. F. Gilchrist, Phys. Rev. E **77**, 025301 (2008).
[21] J. F. Brady and I. E. Carpen, J. Non-Newtonian Fluid Mech. **102**, 219 (2002).
[22] The induction length for shear-induced migration for a tube of radius R and particle size a at 40% concentration is $0.06R^3/a^2$ [19]. For $R = 0.5$ cm and $a = 47$ μm (our largest particle size), the induction length is about 300 cm. For a square tube, the induction length is expected to be higher than this value, because the average length scale in the cross section is greater than 0.5 cm. Since the tube lengths considered in our experiments rarely exceeded 60 cm, any demixing produced by shear-induced migration is negligible. This was also checked by confirming the absence of particle accumulation at the advancing interface when the suspension was drawn up an initially empty square tube.
[23] For the largest particles (94 μm) and lowest volume fraction (30%), the hindered settling velocity can be estimated as $(2/9)\times(47\times10^{-4})^2\times(2.5-1.35)/22.5\times980(1-0.3)^{5.1}\times 10^4\,\mu\mathrm{m/s}\approx0.4\,\mu\mathrm{m/s}$. Typical velocities of the suspension through the square channel were 1 mm/s, which is much larger than the calculated settling velocity noted above. Thus, convection in the flow direction overwhelms the settling of the particles.
[24] S. C. Jana, B. Kapoor, and A. Acrivos, J. Rheol. **39**, 1123 (1995).
[25] J. F. Morris and F. Boulay, J. Rheol. **43**, 1213 (1999).
[26] The excellent agreement with the model using the constitutive equations of Morris and Boulay should be viewed with some reservation, since, in these constitutive equations, the normal stress differences were obtained using the suspension balance model by fitting concentration distributions in viscometric geometries, and not directly from rheological measurements, as was done by Refs. [6–8].
[27] M. K. Lyon and L. G. Leal, J. Fluid Mech. **363**, 25 (1998).
[28] B. Timberlake and J. Morris, J. Fluid Mech. **538**, 309 (2005).
[29] See Supplemental Material at http://link.aps.org/supplemental/10.1103/PhysRevLett.110.018306 for the coextrusion of two concentrated suspensions through a rectangular conduit of aspect ratio 4. It is shown that the interface between the two suspensions is not rectilinear. The experimental trend agrees with a theoretical prediction based on the model employed in this Letter.